International Journal of Heat and Mass Transfer 171 (2021) 121126

Contents lists available at ScienceDirect

International Journal of Heat and Mass Transfer

journal homepage: www.elsevier.com/locate/hmt

Synergy analysis for ion selectivity in nanofluidic salinity gradient energy harvesting

Rui Long*, Mingliang Li, Xi Chen, Zhichun Liu*, Wei Liu

School of Energy and Power Engineering, Huazhong University of Science and Technology, Wuhan 430074, P. R. China

ARTICLE INFO

Article history:
Received 1 December 2020
Revised 26 January 2021
Accepted 16 February 2021

Keywords:
Synergy angle
Synergy degree parameter
Ion selectivity
Nanowire blocker
Salinity gradient energy harvesting

ABSTRACT

For salinity gradient energy harvesting, membrane ion selectivity plays an important role, which is often qualitatively analysed via the electric double layer (EDL) overlapping degree in conventional studies. However, the degree of EDL overlapping is hard to be quantitatively evaluated. Here, we systematically analyze the synergy relations between physical vectors that determining the energy conversion process to quantitatively illustrate the EDL overlapping degree and ion selectivity. Three synergy angles are proposed to describe the synergy relations between the ion diffusion and the electrostatic migration driven forces. A synergy degree parameter is further defined, which could offer a quantitative way to analyze the cation transference number under different concentration ratios, channel length, and asymmetric channel geometries. In addition, an alternative way to use large size nanochannels to efficiently harvest the salinity gradient energy is developed by employing nanowire blockers. The inserted nanowire blocker can significantly enlarge the synergy degree parameter, thus to enhance the ion selectivity, upgrade the membrane potential, and bring a significant augment on the electric power and energy conversion efficiency. This study offers a novel insight into quantitatively analyzing the ion selectivity and paves an alternative way for efficiently salinity gradient energy harvesting via large size nanochannels.

1. Introduction

With increasing energy demand as well as the severe environmental issues caused by fossil fuel combustion, exploring and utilizing clean and renewable energy resources are highly demanded [1,2]. The capacity of salinity gradient energy widely existed in the oceans and rivers reaches about 2.6 TW, about 20% of the world energy consumption worldwide [3]. Efficiently utilization of such energy resources can considerably improve present world energy consumption structure. Reverse electrodialysis (RED) offers a way to utilize the salinity gradient energy [4]. In traditional RED systems, ion exchange membranes (IEMs) are installed to separate the high and low concentration solutions, which allows count-ions passing through and reject co-ions. Driven by the transmembrane concentration gradient, ions diffuse across the IEMs, generating an ionic current, converting the Gibbs free energy of mixing into electricity via an external load [5]. The performance of the traditional RED system is mainly hindered by the sub-1 nm pore sizes in the IEMs [6]. Mimic charged nanochannels, which have a much larger pore size and can offer a much larger ionic current, are developed to function as IEMs. Adjacent to the charged surface, an electric double layer (EDL) is established, which attracts count-ions and repels co-ions. A giant power density of 10^6 has been obtained via a atomically thin MoS_2 membrane [7], illustrating the potential to efficiently harvest the salinity gradient energy.

The performance of the nanofluidic RED systems are mainly depended on membrane characterisers such as nanochannel geometry and surface characteristics, and solution properties such as the temperature, concentration, and pH [8-15]. Various alternative membranes have been developed to improve the energy harvesting performance. Gao et al. [16] employed an asymmetric membrane consisting of negatively charged 7 nm mesoporous carbon and positively charged 80 nm macroporous alumina to harvest the Gibbs free energy of mixing of the artificial seawater and river water, and a power density up to 3.46 W/m^2 was achieved. Li et al. [17] investigated the asymmetric Polymer/MOF hybrid membranes, and a power density of 2.87 W/m^2 was obtained. Guo et al. [18] revealed an electric power of 9.03 μW in a heparin-threaded ZIF-8 membrane. Xin et al. [19] employed a hybrid membrane composed of a silk nanofibril membrane and an anodic aluminum oxide membrane, and a power density of 2.86 W/m^2 is achieved by mixing artificial seawater and river water. Fu et at. [20] fabricated sub-nanometer pores on single-layer graphene and achieved an energy conversion efficiency of 39% and power density of 27 W/m^2 at room temperature. Hong et al. [21] employed lamellar Ti3C2Tx

* Correspondence authors.
E-mail addresses: r_long@hust.edu.cn (R. Long), zcliu@hust.edu.cn (Z. Liu).

https://doi.org/10.1016/j.ijheatmasstransfer.2021.121126
0017-9310/

MXene membranes for efficient osmotic power harvesting, and a power density of 21 W/m^2 with an energy conversion efficiency of 40.6% was obtained at room temperature. Yu et al. [22] used a polypyrrole membrane with asymmetric surface hydrodynamic slip, and an energy density of 1.4 Wh/m^2 was obtained. Graf et al. [23] used light irradiation to augment the surface charge of the MoS_2 membranes, and the osmotic power is increased by 130%.

Tseng et al. [24] found that the electric power increases with increasing temperature while the energy conversion efficiency is insensitive to the temperature variation. To step further, Long et al. [25,26] investigated the impact of asymmetric temperature differences on the energy conversion performance in thermally insulated nanochannel, and found that a counter-diffusion temperature gradient can promote the selectivity and suppresses the ICP, resulting in enhanced membrane potential and electric power. Long et al. [27] further investigate the effects of the membrane thermal conductivity, and proposed a criterion for membrane selection based on membrane thermal conductivities. Tseng et al. [28] conducted an optimization of nanopore size, and found that narrower nanopore and a smaller salt gradient are benefit for a higher efficiency. Cao et al. [29] found that optimal channel length should be between 400 nm and 1000 nm in to achieve a satisfied electric power, while balancing the energy conversion efficiency. Hsu et al. [30] found in highly charged nanochannels, the performance of osmotic power decreases with increasing surface charge density for significantly augmented ion concentration polarization effect.

The synergy relations between the physical vectors can reflect the process performance to some extent. In the convective heat transfer enhancement, the flow and heat transfer characteristics are described by the Navier-Stocks equation and energy conservation equation. The driven forces for the processes are often illustrated via physical vectors such as the velocity, pressure gradient and temperature gradient. Guo et al. [31] proposed a novel insight into the heat transfer enhancement via analysing the synergy angle between velocity and the temperature gradient. The better the synergy between velocity and temperature gradient, the better the heat transfer performance [32,33]. Liu et al. [34,35] analysed the synergy angle between the pressure gradient and the velocity, and found the better the synergy between velocity and pressure gradient, the less flow power consumption. For the ion transportation in the salinity gradient harvesting system, the ion transportation characteristic can be illustrated by the Poisson-Nernst-Planck (PNP) equations, driven by the electrostatic and diffusive forces. The performance can be reflected by the synergy angles between the cation/anion concentration gradient and the electric field. Relevant studies have never been conducted. It's highly demanded to analyze the synergy relations in determining the performance of the nanofluidic salinity gradient harvesting systems.

For salinity gradient energy harvesting, membrane ion selectivity plays an important role, which is often qualitatively analysed via the electric double layer (EDL) overlapping degree in conventional studies. However, the EDL overlapping degree is hard to be quantitatively evaluated. Here, we systematically analyze the synergy relations between the physical vectors that determining the energy conversion process. For mono-component solutions, we proposed three synergy angles α, β and γ to describe the synergy relations between the ion diffusion and the electrostatic migration driven forces. To step further, we proposed a synergy degree parameter to quantitatively analyze the ion selectivity for different geometry configurations based on the proposed synergy angles. The synergy analysis is conducted in evaluating the EDL overlapping degree and ion selectivity under different concentration ratios, channel length, and asymmetric channel geometries. In addition, an alternative way to use traditional large nanochannels, which are recognized not suitable for osmotic energy harvesting, to efficiently harvest the salinity gradient energy is developed via employing nanowire blockers. The nanowire blocker can significantly enlarge the synergy degree parameter, thus to enhance the ion selectivity, upgrade the membrane potential, and bring a significant augment on the electric power and energy conversion efficiency. This study offers a novel insight into quantitatively analyzing the ion selectivity and paves an alternative way for efficiently salinity gradient energy harvesting via large size nanochannels.

2. Results and discussion

2.1. Synergy principle in evaluating ion selectivity

The Poisson-Nernst-Planck (PNP) equations as well as the Navier-Stocks equations are widely employed to model the electrostatics and ionic mass transport in the salinity gradient energy harvesting, which are given by [13,26,27,36]

$$-\varepsilon\nabla^2\varphi = F\sum z_i c_i \tag{1}$$

$$\nabla\cdot\vec{J_i} = 0 \text{ where} \vec{J_i} = c_i\vec{u} - D_i\nabla c_i - \frac{D_i z_i F c_i}{RT}\nabla\varphi \tag{2}$$

$$-\nabla p + \mu\nabla^2\vec{u} - F\sum z_i c_i\nabla\varphi = 0 \tag{3}$$

$$\nabla\cdot\vec{u} = 0 \tag{4}$$

where φ is the electrical potential. $\vec{J_i}$, c_i,$D_i$and z_i are the ionic flux, concentration, diffusivity, and valence of the ith ionic species, respectively ($i = 1$ for cation and $i = 2$ for anion in present study). F, R and T are the Faraday constant, universal gas constant and temperature. ε, p, and $\vec{u}$are the solution permittivity, pressure, and velocity. To solve above equations, appropriate boundary conditions are needed [37]. The validation of present model can been see in our previous literatures [26,27]. The electric current through the nanopore, I, is calculated as $I = \int_\Lambda F(\sum_i^2 z_i\vec{J_i})\cdot\vec{n}d\Lambda$, where Λ represents either ends of the reservoirs. The cation transference number $t+$ evaluating the ion selectivity can be calculated as $t^+ = I^+/(I^+ + |I^-|)$, where I^+ and I^- represents the ionic current contributed by the cations and anions.

Provided the nanochannel is much longer than the radius and the ionic profile inside the pore is in local equilibrium in radial direction, based on Eq. (2), we have [38,39]

$$\frac{\partial c_i(x,r)}{\partial r} = -\frac{\partial\varphi(x,r)}{\partial r}\frac{z_i F c_i(x,r)}{RT} \tag{5}$$

Implement Eq. (6) in Eq. (1) yields to [39]

$$\varepsilon\nabla^2\varphi(x,r) = RT\sum\frac{\partial c_i(x,r)}{\partial r}\Big/\frac{\partial\varphi(x,r)}{\partial r} \tag{6}$$

Based on Eqs. (6) and (7), there exist synergy relations between the driven forces: reverse concentration gradient $-\nabla c_i$ and the reverse potential gradient$-\nabla\varphi$. For mono-component solutions, the synergy relations between the reverse gradients $-\nabla c_1$, $-\nabla c_2$, and the electric field $E = -\nabla\varphi$ can be expressed by the following synergy angles:

$$\alpha = \arccos\frac{\nabla c_1\cdot\nabla c_2}{|\nabla c_1||\nabla c_2|} \tag{7}$$

$$\beta = \arccos\frac{\nabla c_1\cdot\nabla\varphi}{|\nabla c_1||\nabla\varphi|} \tag{8}$$

$$\gamma = \arccos\frac{\nabla c_2\cdot\nabla\varphi}{|\nabla c_2||\nabla\varphi|} \tag{9}$$

Meanwhile, in Eq. (2), the convective item can be ignored due to relative small contribution [29]. As shown in Fig. 1a, the ionic

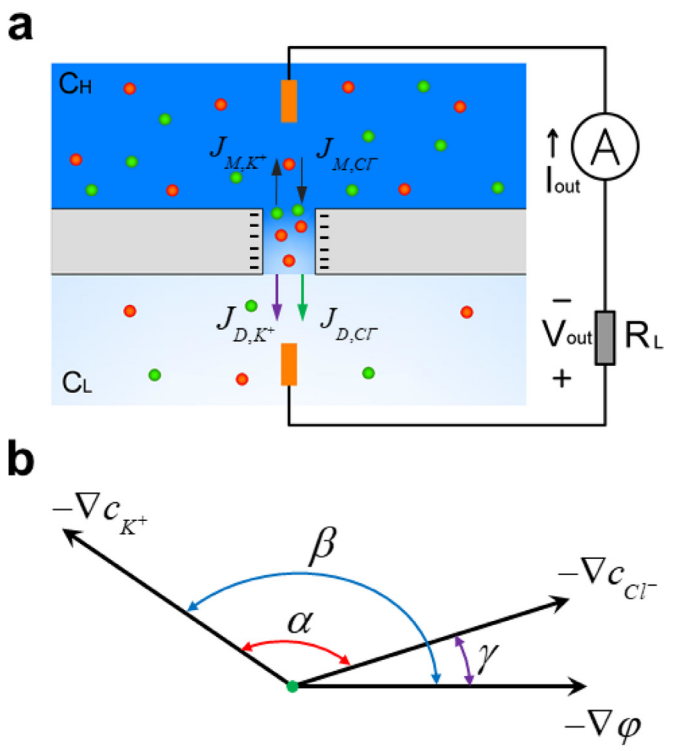

Fig. 1. Schematic diagram of the K^+ and Cl^- transportation (a) and three synergy angles α, β, and γ (b) to describe the synergy relations between the reverse gradients $-\nabla c_{K^+}$, $-\nabla c_{Cl^-}$, and $-\nabla\varphi$ for salinity gradient harvesting via a two-dimensional or cylindrical nanochannel, where c is the ion concentration, φ is the potential.

current mainly consists of the ion diffusion and the electrostatic migration, which can be illustrated by

$$I = F\int_{\Lambda}\left[\left(\underbrace{J_{D,K^+}-J_{D,Cl^-}}_{Diffusion}\right)-\left(\underbrace{J_{M,K^+}+J_{M,Cl^-}}_{Migration}\right)\right]d\Lambda \tag{10}$$

As shown in Fig. 1b, α denotes the synergy angle between the reverse concentration gradients of the cation and anion, which reflects the diffusion synergy relation of the cations and anions. In the salinity gradient energy harvesting, driven by the concentration gradient, ions diffuse across the nanopore. To guarantee a local equilibrium state, an electric field is established to compensate the ion diffusion [40]. The ion flux mainly consists of the ion diffusion and ion migration, and the ion distributions are determined by the electrostatic interaction and ion diffusion. A lagerαapproaching 180° means cation and anion diffuse in the opposite direction, which originates from the impact of significant EDL overlapping. Therefore, α can reflect the distribution of spatial EDL overlapping degree. Larger α means better charge separation and higher ion selectivity. β and γ denotes the synergy angles between the reverse cation/anion concentration gradient and the electrical filed, which reflect the synergy relation of the ion diffusion and migration. Due to opposite sign of the cation and anion, the cation migration by the electric force is in the same direction as the electric field while the anion migration is in the opposite direction as the electric field. For a negative charged nanopore, the ionic current direction is the same as the cation transportation direction. A large β approaching 180 and a small γ approaching 0 indicate that the ion diffusion is well compensated by the electrostatic force, indicating that a satisfied electric field is established. For a two-dimensional or cylindrical nanochannel, β=α+γ. We define a parameter ω=α/β to evaluate synergy degree of the ion diffusion and electric migration. The synergy degree parameter ω approaching 1 means, the cation and anion is well separated under the electric field, revealing the significant EDL overlapping degree and desired ion selectivity.

Here we conduct a synergy analysis on the selectivity of a negatively charged cylindrical nanopore under various concentration ratios and channel length. The inner surface is maintained at a constant charge $\sigma = -60mC/m^2$ [41]. The nanochannel connects two same large reservoirs (KCl aqueous solution) of R_r=1000 nm and length L_r=1000 nm. The channel length L varies from 50 nm to 2000 nm, and the transmembrane concentration ratio varies from 3 to 1000 with the low concentration fixed at 1 mM. The calculation is conducted via the COMSOL software, and the average synergy angles are obtained in the space-averaged manner in the nanopore interior. Fig. 2 depicts the average synergy angles under different concentration ratios and channel length. Higher concentration weakens the EDL overlapping degree. α and β decrease with increasing concentration ratios, while γ increases. With increasing channel length, the ion polarization is much weakened, the EDL overlapping degree is enhanced [26,29]. The ion aggregation and depletion are more obvious in the nanopore interior. Therefore, αincreases with increasing channel length. The variation of β with channel length is concentration depended. At low concentration ratios, the EDL overlapping degree is significant in entire nanopore interior where the charges can be well separated. Increasing channel length increases β. At high concentration ratios, the EDL overlapping degree is much weak at the nanopore inlet and more significant at the nanopore outlet [26]. For a short channel, the EDL overlapping degree is much deteriorated as strong ion polarization [29]. A short channel length contributes to transmembrane concentration gradient that enhances the ion diffusion. Due to impact of unequal mobilities of the anion and cation, the synergy angle between the cation and induced electrical field is at a relatively large value, which decrease with increasing channel length for weakened concentration gradient. For a long channel, the ion polarization is weakened, and the EDL overlapping degree is significant. Increasing channel length increases the synergy angle β. As longer channel length augments the EDL overlapping degree, which considerably repels anion, leading to decreased γ.

The EDL overlapping degree can be evaluated by synergy angle α between the reverse concentration gradients of the cation and anion. As shown in Fig. 3, higher concentration ratio deteriorates the EDL overlapping degree and decreases the synergy angle α, leading to lowered ion selectivity. Much larger synergy angle α is observed at the low concentration side for a long channel, comparing to that under the short nanochannel, indicating that the EDL overlapping degree is much significant under the long nanochannel, resulting in upgraded ion selectivity. The synergy degree parameter ω exhibits the same trend with the ion selectivity, which evaluates synergy degree of the ion diffusion and electric migration. ωapproaching 1 means, the cation and anion is well separated under the electric filed. The larger concentration ratio, the smaller ω and lower selectivity. The longer channel length, the larger ω and higher selectivity.

To step further, we conduct a synergy analysis on the selectivity of the asymmetric conical nanopore. The pore length is 600 nm. The inner surface is maintained at a constant charge $\sigma = -60mC/m^2$. The transmembrane concentration ratio varies from 3 to 1000 with the low concentration fixed at 1 mM. Fig. 4 depicts the average synergy angles in the nanopore interior under different concentration ratios. As the asymmetric nature of the conical nanopore, the energy harvesting system takes in two configuraitons: low concenration applied at base side (Conf. I) or low concentration at the tip side (Conf. II). In both configurations, the average synergy angle α and β both decreases with increasing concentration ratios while γ increases for weakened EDL overlapping degree under high concentrations. As shown in Fig. 4c, in Conf. I

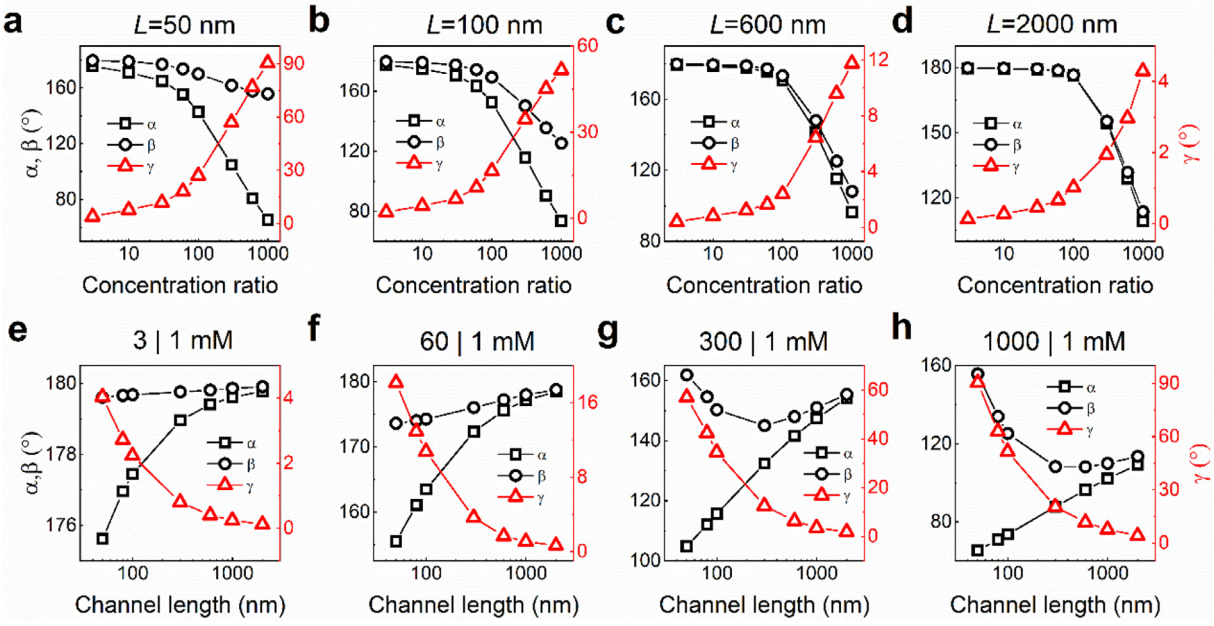

Fig. 2. Average synergy angles in the nanopore interior under different concentration ratios (a-d) and channel length *L* (d-f).

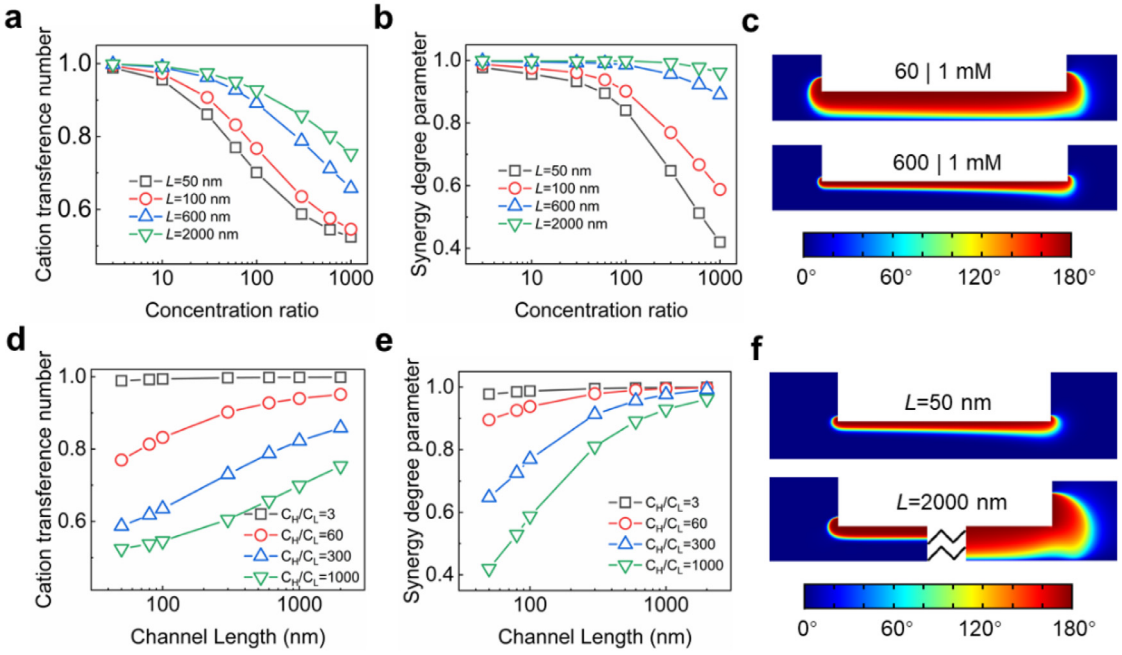

Fig. 3. Cation transference number and synergy degree parameter under different concentration ratios (a, b) and channel length (d,e). Distribution of α at high and low concentration ratios (c), and at short and long channel length (f).

with high cocencentration solution applied at the tip side, charges are separated in the entire nanopore, while in Conf. II with high concentration solution applied at the base side, obvious charge separation only exists near the low concentration tip end. Therefore, the average synergy angle αin Conf. II are small than those under the opposite configuration. However, as shown in Fig. 4e, the cation transference number in Conf. II is larger than that in Conf. I. Impacted by the asymmetric geometry, the averaged synergy angle αcould not accurately reflect the charge separation in asymmetric geometries. Here we analyze the distribution of synergy angel α at the low concentration side, as shown in Fig. 4d. The synergy angle$\alpha$with large values almost occupy the entire outlet section in the Conf. II, indicating the ion separation is much obvious, resulting in upgraded ion selectivity. We further compare the synergy degree parameter ω under these two configurations. We can see that the synergy degree parameter ω can well distinguish the cation transference number under different configurations, as depicted in Fig. 4f. Under various concentration ratios, the larger ω, the better ion selectivity.

According to the aformationed analysis, the synergy angle α distribution at the low concentration end can be employed to describe the EDL overlapping degree and qualitatively analyze the ion selectivity. ω can serve as a quantitative criterion for evaluating the ion selectivity and identifying preferred system configurations.

To step further, we employ the machine learning method to establish a quantitative relationship between the synergy angle and

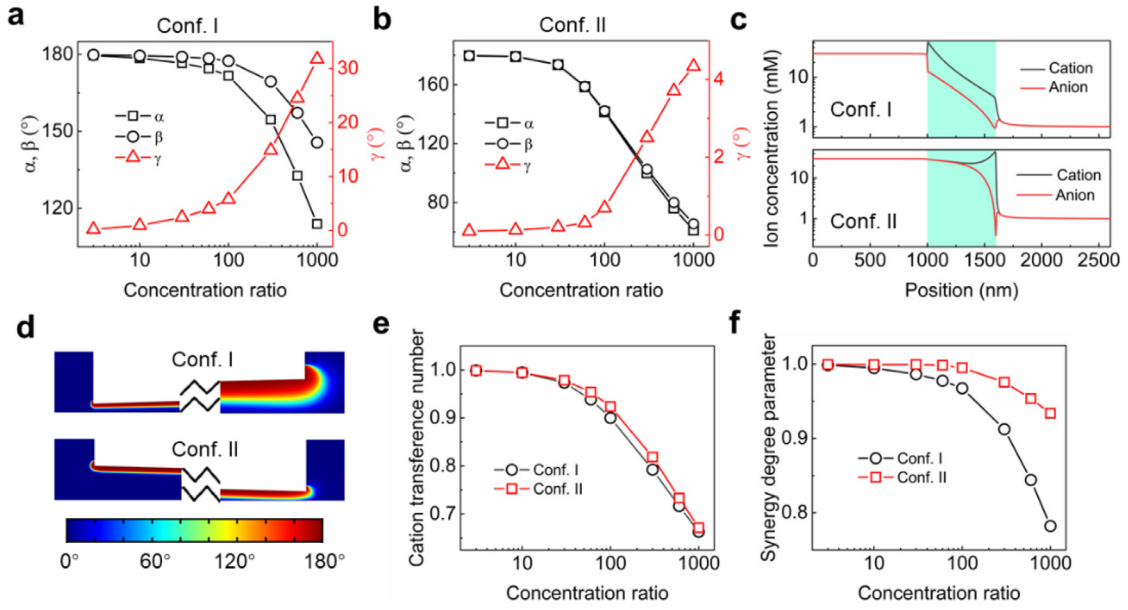

Fig. 4. Average synergy angles in the nanopore interior (a, b), axial ion concentration (c), distribution of α at a concentration ratio of 600-fold (d), transference numberunder (e), and synergy degree parameter (f) under different concentration ratios for different system configurations.

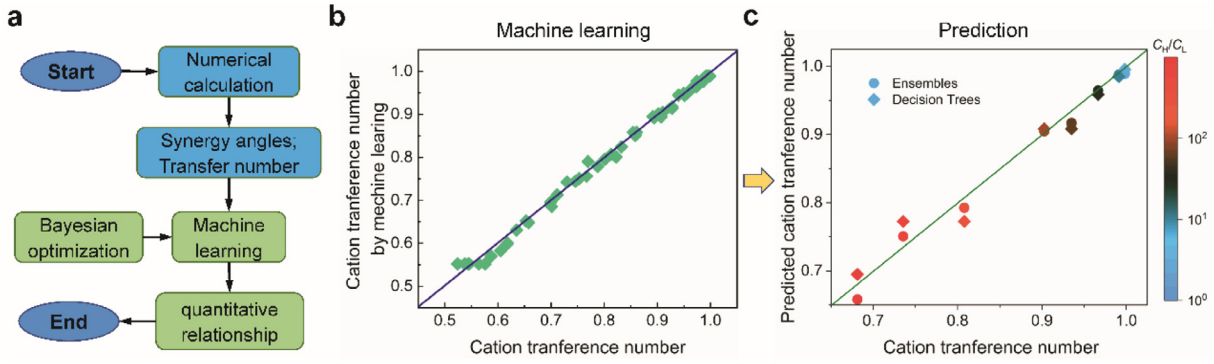

Fig. 5. (a) Flowchart for the machine learning procedure; (b) Comparison between predicted and calculated ion selectivity during the ensemble-based machine learning process; (c) Prediction of the cation transference number based on the obtained quantitative relationship between the synergy angle and the ion selectivity.

Table 1
Accuracy of the employed machine learning models.

Machine learning models	RSME	R^2	MSE	MAE
Decision trees	0.041854	0.93	0.0017518	0.030302
Ensembles	0.025312	0.97	0.00064071	0.018578

the ion selectivity in cylindrical channels. As shown Fig. 5a, machine learning based on decision trees and ensembles are conducted, where Bayesian optimization is employed to obtain the optimal hyper-parameters of the machine learning models [42]. Both machine learning models are trained several times with 5-fold cross-validation to alleviate the random error and acquire the hidden quantitative relationship between the synergy angles and cation transference number. Root mean square error (RMSE), R^2, MAE (mean absolute error), MSE (mean square error) are adopted to describe the model accuracy (See Table 1). The obtained relationship between the synergy angles and ion selectivity is further used for prediction for ion selectivity in nanochannel at length equal to 800 nm under various concentration ratios, and great accordance has been encountered. Both the decision tree and ensemble models can successfully predict the ion selectivity, while the ensemble-based machine learning model present higher accuracy, especially under large transmembrane concentration ratios, as depicted in Fig. 5.

3.2. Nanowire-enhanced energy generation

Generally, nanopores with large sizes are nor suitable for salinity gradient energy harvesting for extremely weak EDL overlapping degree. Recent advances in nanotechnology and material science makes it possible to fabricate nanowire with radius of nanometers. Here we propose an alternative way to use the large size nanochannel via nanowire blockers for efficient salinity gradient energy harvesting, as shown in Fig. 6. The inner surface of the nanopore is maintained at a constant charge $\sigma = -80mC/m^2$. The nanochannel of length $L = 200$ nm and radius $R = 40$ nm connects two same large reservoirs (KCl aqueous solution) of radius R_r=1000 nm and length L_r=1000 nm. The nanopore interior is blocked by a nanowire blocker, whose radius varies from 10 nm to 35 nm. The nanowire is free of charge. The transmembrane concentration ratio varies from 3 to 1000 with the low concentration fixed at 1 mM.

As shown in Fig. 7, the cation transference number with/out nanowire blockers decreases with increasing concentration ratios for thinned EDL at high concentration ratios. As the existence of

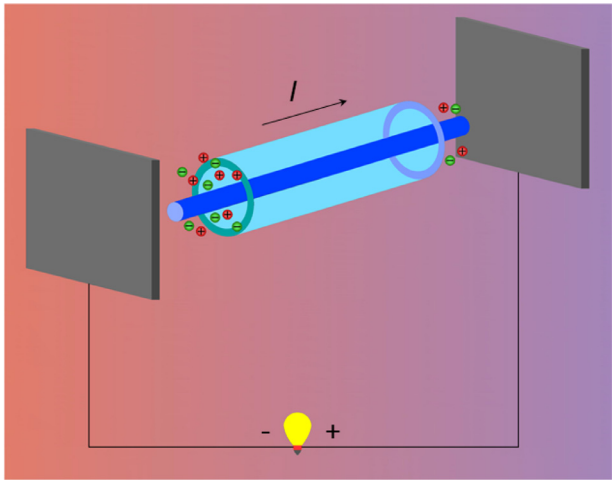

Fig. 6. Schematic diagram of the large size nanochannel via nanowire blockers for efficient salinity gradient energy harvesting.

the nanowire blocker, ions are forced to diffuse more close to the EDL impacted zone, where the ion transportation is significantly impacted by the EDL. Therefore, charges can be well separated, as depicted in Fig. 7b. Here, we employ the synergy degree parameter proposed in the previous section to evaluate the cation transference number. We can see that under different concentration ratios, the synergy degree parameter increases with increasing size of the nanowire blocker, indicating upgraded ion selectivity.

Fig. 8a and b depict the osmotic current, membrane potential under different nanowire blocker sizes for various concentration ratios. The osmotic current first increases with increasing concentration ratios, reaches its maximum value then decreases. At low concentration ratios, the EDL is much thicker. Increasing transmembrane concentration ratio contributes more K^+ passing through the nanochannel interior, leading to augmented osmotic current. High concentration thins the EDL, and the transmembrane concentration gradient is strong, facilitating the transport of Cl^-, resulting in decreased osmotic current. Larger nanowire blocker size contributes to the osmotic current for more significant charge separaiton in the nanochannel interior, as shown in Fig. 8c. The membrane potential is extracted from the *I-V* curves [36,43]. Due to the compromise between the ion selectivity and the concentration ratio, the membrane potential increases with increasing concentration raito first, achieves its maximum value, then decreases [37]. Larger nanowire blocker size renders higher ion selectivity, thus larger membrane potential.

Fig. 8c and d show the maximum electric power and the coresponding energy conversion efficiency under different nanowire blocker sizes for various concentration ratios. Orignating from the compromise between the osmotic current and membrane potential, there exists a maximum electric power when the concentration ratio increases. The electric power can be significantly improved with nanowire blocker employed. As shown in Fig. 8a, at a concentration of 100-fold, compared to the original nanochannel, the electric power with 35 nm nanowire blocker is elevated by 362%. The energy conversion efficiency according to the maiximum electric power can be calculated as $\eta = (2t^+ - 1)^2/2$. The nanowire blocker improves the ion selectivtiy, thus upgrades the energy conversion efficiency. We further investigate the impact of charged

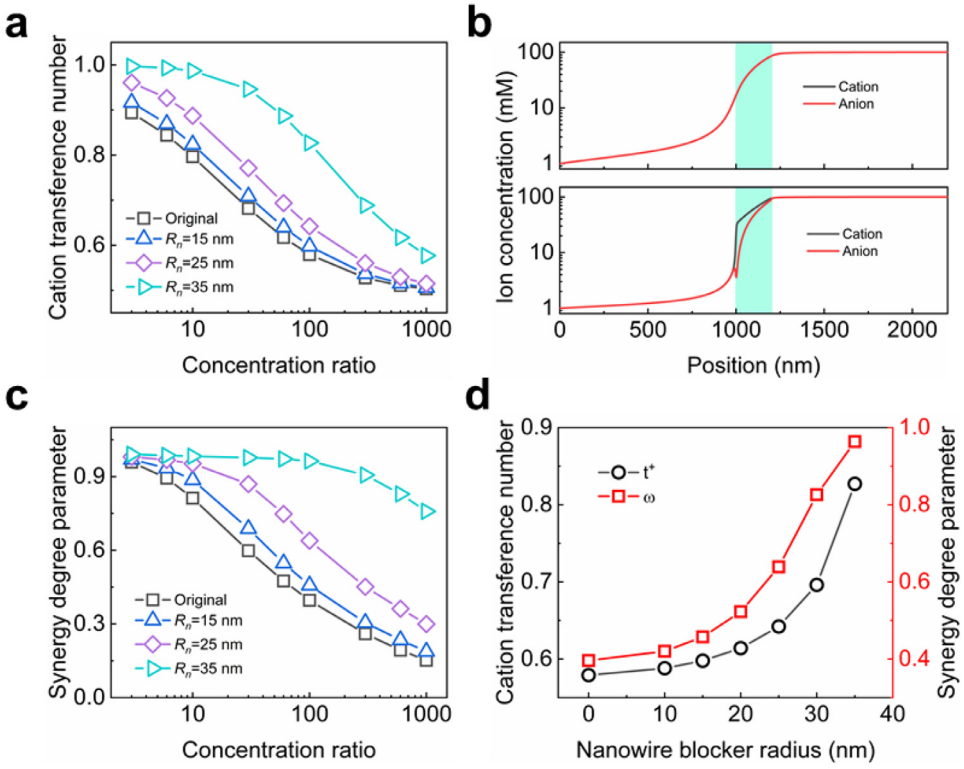

Fig. 7. Cation transference number (a) under different nanowire blocker sizes for various concentration ratios; (b) Axial ion concentration for the original nanopore and the that on the nanowire surface, where the concentration ratio is 100-fold and the nanowire radius is 35 nm. (c) Synergy degree parameter (c) under different nanowire blocker sizes for various concentration ratios; (d) Cation transference number and synergy degree parameter under different nanowire sizes, where the concentration ratio is 100-fold.

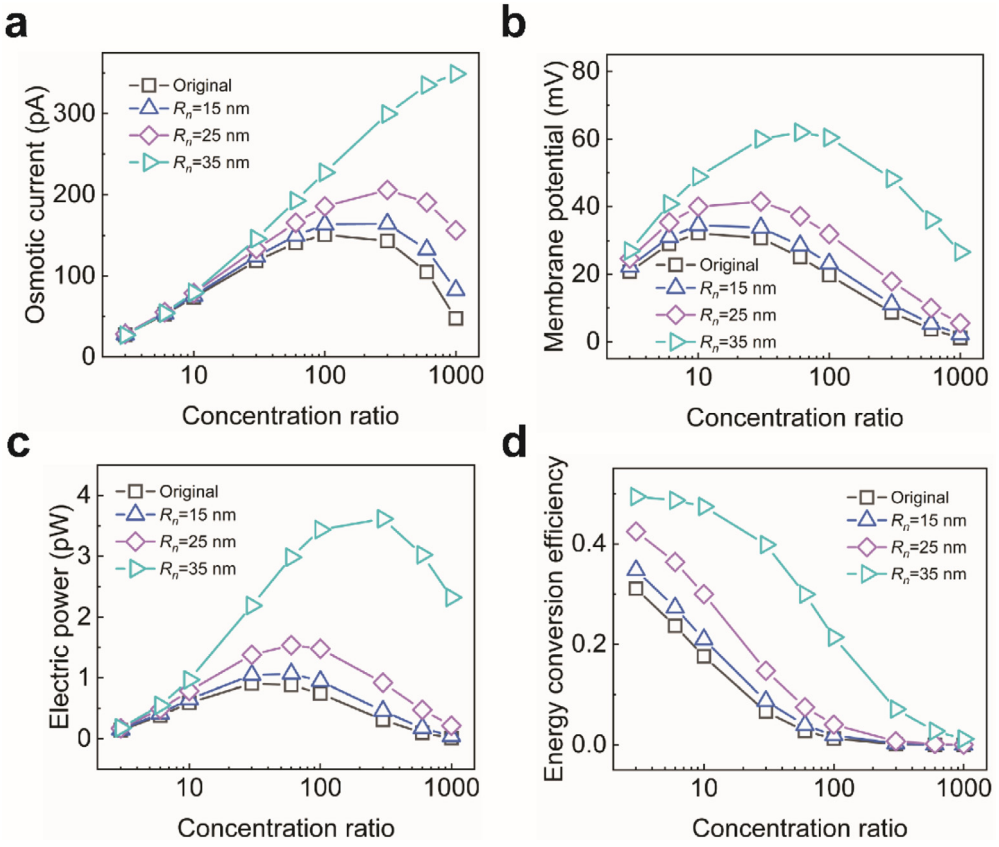

Fig. 8. Osmotic current (a), membrane potential (b), electric power (c) and energy conversion efficiency (d) under different nanowire blocker sizes for various concentration ratios.

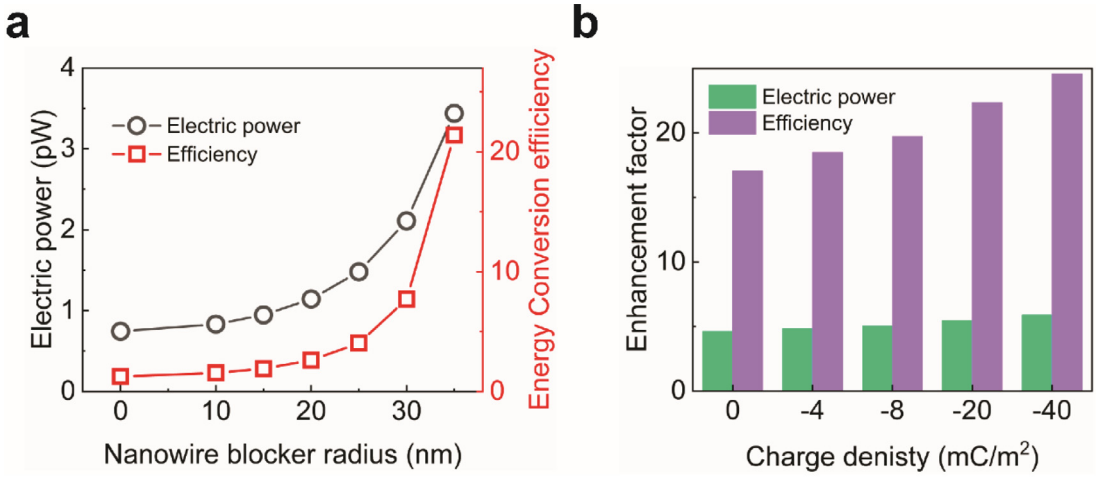

Fig. 9. (a) Electric power and the energy conversion efficiency under different nanowire blocker sizes; (b) Performance enhancement factor under different surface charge density of nanowire blocker with radius R_n=35 nm. The performance enhancement factor is calculated by the power/energy conversion efficiency with nanowire blocker divided by that obtained in the original nanochannel. In the calculation, the transmembrane concentration ratio is 100-fold.

nanowire blocker on the energy converison performance. The performance enhancement factor is calculated by the power/energy conversion efficiency with nanowire blocker divided by that obtained in the original nanochannel. At a concentration of 100-fold, the energy conversion efficiency with 35 nm nanowire blocker is about 17 times to that under the original nanochannel. If the nanowire surface is modified with charges, a furhter improvement of the energy harvesting peroformance elevation can be obtained, as depicted in Fig. 9b.

As additional remarks, recent advances in nanotechnology and fabrication enable fabricating nanowires with larger sizes with diameter about 100 nm via the bottom-up approaches such as vapor–liquid–solid growth, supercritical fluid liquid solid, and laser ablation [44]. Sub-20 nm Si nanowires can also be achieved via chemical ethhing and thermal oxidation [45]. To scale up, the mesoscopic nanochannel can also be employed to harvest the osmotic power with nanowire array or mesoscopic blockers. Privided the blocker surface is modifide with surface charges, a significant

elevation to the salinity gradient energy harvesitng performace can be desired.

4. Conclusions

In conclusion, the synergy relations between the physical vectors that determining the energy conversion process for salinity gradient energy harvesting are systematically investigated. For mono-component solutions, we proposed three synergy angles α, β, and γ to describe the synergy relations between the ion diffusion and the electrostatic migration driven forces, which reflect the EDL overlapping degree. A synergy degree parameter is further defined, which can quantitatively illustrate the EDL overlapping degree and ion selectivity under different concentration ratios, channel length, and asymmetric channel geometries. In addition, an alternative way to use large size nanochannels, which are recognized not suitable for osmotic energy harvesting, to efficiently harvest the salinity gradient energy is developed by employing nanowire blockers. The ion selectivity is evaluated based on the synergy degree parameter. The nanowire blocker can significantly enhance the ion selectivity, upgrade the membrane potential, thus to bring a significant augment on the electric power and energy conversion efficiency. At a concentration of 100-fold, compared to the original nanochannel, the electric power and energy conversion efficiency with 35 nm nanowire blocker are elevated by 362% and 1603.4%, respectively. It should be mentioned that although the synergy angles cannot be obtained before the numerical analysis, the proposed synergy angels represent the synergy relationship between the ion diffusion driven force and the electrostatic driven force in the transmembrane ion transportation, which could provide an alternative perspective for analyzing the transmembrane ion transportation in salinity gradient energy harvesting.

Declaration of competing interest

The authors declare no competing financial interest.

CRediT authorship contribution statement

Rui Long: Conceptualization, Writing – original draft. **Mingliang Li:** Visualization, Investigation. **Xi Chen:** Formal analysis. **Zhichun Liu:** Conceptualization. **Wei Liu:** Writing – review & editing.

Acknowledgements

This work was financially supported by the National Natural Science Foundation of China (52076088).

References

[1] R. Long, B. Li, Z. Liu, W. Liu, Hybrid membrane distillation-reverse electrodialysis electricity generation system to harvest low-grade thermal energy, J. Memb. Sci. 525 (2017) 107–115.
[2] R. Long, F. Wu, X. Chen, Z. Liu, W. Liu, Temperature-depended ion concentration polarization in electrokinetic energy conversion, Int. J. Heat Mass Transf. 168 (2021) 120842.
[3] L. Cao, W. Guo, W. Ma, L. Wang, F. Xia, S. Wang, Y. Wang, L. Jiang, D. Zhu, Towards understanding the nanofluidic reverse electrodialysis system: well matched charge selectivity and ionic composition, Energy Environ. Sci. 4 (2011) 2259–2266.
[4] Z. Kuang, D. Zhang, Y. Shen, R. Long, Z. Liu, W. Liu, Bioinspired fractal nanochannels for high-performance salinity gradient energy conversion, J. Power Sources. 418 (2019) 33–41.
[5] D. Pintossi, M. Saakes, Z. Borneman, K. Nijmeijer, Electrochemical impedance spectroscopy of a reverse electrodialysis stack: a new approach to monitoring fouling and cleaning, J. Power Sources. 444 (2019) 227302.
[6] T. Okada, G. Xie, O. Gorseth, S. Kjelstrup, N. Nakamura, T. Arimura, Ion and water transport characteristics of Nafion membranes as electrolytes, Electrochim. Acta. 43 (1998) 3741–3747.
[7] J. Feng, M. Graf, K. Liu, D. Ovchinnikov, D. Dumcenco, M. Heiranian, V. Nandigana, N.R. Aluru, A. Kis, A. Radenovic, Single-layer MoS2 nanopores as nanopower generators, Nature 536 (2016) 197–200.
[8] T. Ma, E. Balanzat, J.M. Janot, S. Balme, Nanopore Functionalized by Highly Charged Hydrogels for Osmotic Energy Harvesting, ACS Appl. Mater. Interfaces. 11 (2019) 12578–12585.
[9] Q. Wu, C. Wang, R. Wang, C. Chen, J. Gao, J. Dai, D. Liu, Z. Lin, L. Hu, Salinity–Gradient Power Generation with Ionized Wood Membranes, Adv. Energy Mater. 1902590 (2019) 1902590.
[10] D.J. Rankin, D.M. Huang, The Effect of Hydrodynamic Slip on Membrane-Based Salinity-Gradient-Driven Energy Harvesting, Langmuir 32 (2016) 3420–3432.
[11] H. Li, F. Xiao, G. Hong, J. Su, N. Li, L. Cao, Q. Wen, W. Guo, On the Role of Heterogeneous Nanopore Junction in Osmotic Power Generation, Chinese J. Chem. 37 (2019) 469–473.
[12] J.P. Hsu, S.C. Lin, C.Y. Lin, S. Tseng, Power generation by a pH-regulated conical nanopore through reverse electrodialysis, J. Power Sources. 366 (2017).
[13] L.H. Yeh, F. Chen, Y.-T.T. Chiou, Y.-S.S. Su, Anomalous pH-Dependent Nanofluidic Salinity Gradient Power, Small 13 (2017) 1702691.
[14] J.P. Hsu, S.T. Yang, C.Y. Lin, S. Tseng, Voltage-controlled ion transport and selectivity in a conical nanopore functionalized with pH-tunable polyelectrolyte brushes, J. Colloid Interface Sci. 537 (2019) 496–504.
[15] A.M. Benneker, H.D. Wendt, R.G.H. Lammertink, J.A. Wood, Influence of temperature gradients on charge transport in asymmetric nanochannels, Phys. Chem. Chem. Phys. 19 (2017) 28232–28238.
[16] J. Gao, W. Guo, D. Feng, H. Wang, D. Zhao, L. Jiang, High-performance ionic diode membrane for salinity gradient power generation, J. Am. Chem. Soc. 136 (2014) 12265–12272.
[17] R. Li, J. Jiang, Q. Liu, Z. Xie, J. Zhai, Hybrid nanochannel membrane based on polymer/MOF for high-performance salinity gradient power generation, Nano Energy 53 (2018) 643–649.
[18] Y. Guo, H. Huang, Z. Li, X. Wang, P. Li, Z. Deng, X. Peng, Sulfonated Sub–Nanochannels in a Robust MOF Membrane: harvesting Salinity Gradient Power, ACS Appl. Mater. Interfaces. 11 (2019) 35496–35500.
[19] W. Xin, Z. Zhang, X. Huang, Y. Hu, T. Zhou, C. Zhu, X.-Y. Kong, L. Jiang, L. Wen, High-performance silk-based hybrid membranes employed for osmotic energy conversion, Nat. Commun. 10 (2019) 3876.
[20] Y. Fu, X. Guo, Y. Wang, X. Wang, J. Xue, An atomically-thin graphene reverse electrodialysis system for efficient energy harvesting from salinity gradient, Nano Energy 57 (2019) 783–790.
[21] S. Hong, F. Ming, Y. Shi, R. Li, I.S. Kim, C.Y. Tang, H.N. Alshareef, P. Wang, Two-Dimensional Ti3C2Tx MXene Membranes as Nanofluidic Osmotic Power Generators, ACS Nano 13 (2019) 8917–8925.
[22] C. Yu, X. Zhu, C. Wang, Y. Zhou, X. Jia, L. Jiang, X. Liu, G.G. Wallace, A smart cyto-compatible asymmetric polypyrrole membrane for salinity power generation, Nano Energy 53 (2018) 475–482.
[23] M. Graf, M. Lihter, D. Unuchek, A. Sarathy, J.P. Leburton, A. Kis, A. Radenovic, Light-enhanced blue energy generation using MoS2 nanopores, Joule 3 (2019) 1549–1564.
[24] S. Tseng, Y.M. Li, C.Y. Lin, J.P. Hsu, Salinity gradient power: influences of temperature and nanopore size, Nanoscale 8 (2016) 2350–2357.
[25] R. Long, Z. Kuang, Z. Liu, W. Liu, Temperature regulated reverse electrodialysis in charged nanopores, J. Memb. Sci. 561 (2018) 1–9.
[26] R. Long, Z. Kuang, Z. Liu, W. Liu, Ionic thermal up-diffusion in nanofluidic salinity-gradient energy harvesting, Natl. Sci. Rev. 6 (2019) 1266–1273.
[27] R. Long, Z. Luo, Z. Kuang, Z. Liu, W. Liu, Effects of heat transfer and the membrane thermal conductivity on the thermally nanofluidic salinity gradient energy conversion, Nano Energy 67 (2020) 104284.
[28] S. Tseng, Y.M. Li, C.Y. Lin, J.P. Hsu, Salinity gradient power: optimization of nanopore size, Electrochim. Acta. 219 (2016) 790–797.
[29] L. Cao, F. Xiao, Y. Feng, W. Zhu, W. Geng, J. Yang, X. Zhang, N. Li, W. Guo, L. Jiang, Anomalous Channel-Length Dependence in Nanofluidic Osmotic Energy Conversion, Adv. Funct. Mater. 27 (2017) 1604302.
[30] J.-P. Hsu, T.-C. Su, P. Peng, S.-C. Hsu, M. Zheng, L. Yeh, Unraveling the Anomalous Surface-Charge-Dependent Osmotic Power Using a Single Funnel-Shaped Nanochannel, ACS Nano 13 (2019) 13374–13381.
[31] Z.Y. Guo, D.Y. Li, B.X. Wang, A novel concept for convective heat transfer enhancement, Int. J. Heat Mass Transf. 41 (1998) 2221–2225.
[32] Z.Y. Guo, W.Q. Tao, R.K. Shah, The field synergy (coordination) principle and its applications in enhancing single phase convective heat transfer, Int. J. Heat Mass Transf. 48 (2005) 1797–1807.
[33] Q. Chen, J. Ren, J. Meng, Field synergy equation for turbulent heat transfer and its application, Int. J. Heat Mass Transf. 50 (2007) 5334–5339.
[34] W. Liu, Z. Liu, Z. Guo, Physical quantity synergy in laminar flow field of convective heat transfer and analysis of heat transfer enhancement, Chinese Sci. Bull. 54 (2009) 3579.
[35] W. Liu, P. Liu, Z.M.M. Dong, K. Yang, Z.C.C. Liu, A study on the multi-field synergy principle of convective heat and mass transfer enhancement, Int. J. Heat Mass Transf. 134 (2019) 722–734.
[36] L.-H. Yeh, Z.-Y. Huang, Y.-C. Liu, M.-J. Deng, T.-H. Chou, H.-C. Ou Yang, T. Ahamad, S.M. Alshehri, K.C.-W. Wu, A nanofluidic osmotic power generator demonstrated in polymer gel electrolytes with substantially enhanced performance, J. Mater. Chem. A. 7 (2019) 26791–26796.
[37] R. Long, Z. Kuang, Z. Liu, W. Liu, Reverse electrodialysis in bilayer nanochannels: salinity gradient-driven power generation, Phys. Chem. Chem. Phys. 20 (2018) 7295–7302.

[38] W.-H. Koh, J.L. Anderson, Electroosmosis and electrolyte conductance in charged microcapillaries, AIChE J 21 (1975) 1176–1188.
[39] P.B. Peters, R. Van Roij, M.Z. Bazant, P.M. Biesheuvel, Analysis of electrolyte transport through charged nanopores, Phys. Rev. E. 93 (2016) 1–14.
[40] S. Qian, B. Das, X. Luo, Diffusioosmotic flows in slit nanochannels, J. Colloid Interface Sci. 315 (2007) 721–730.
[41] Y. Ma, L.H. Yeh, S. Qian, PH-regulated ionic conductance in a nanopore, Electrochem. Commun. 43 (2014) 91–94.
[42] R. Long, X. Xia, Y. Zhao, S. Li, Z. Liu, W. Liu, Screening metal-organic frameworks for adsorption-driven osmotic heat engines via grand canonical Monte Carlo simulations and machine learning, IScience 24 (2021) 101914.
[43] M. Gao, P.-C. Tsai, Y.-S. Su, P.-H. Peng, L.-H. Yeh, Single Mesopores with High Surface Charges as Ultrahigh Performance Osmotic Power Generators, Small 16 (2020) 2006013.
[44] K. Das, S. Mukherjee, S. Manna, S.K. Ray, A.K. Raychaudhuri, Single Si nanowire (diameter $\leq$ 100 nm) based polarization sensitive near-infrared photodetector with ultra-high responsivity, Nanoscale 6 (2014) 11232–11239.
[45] L. Li, Y. Fang, C. Xu, Y. Zhao, N. Zang, P. Jiang, K.J. Ziegler, Fabricating vertically aligned sub-20 nm Si nanowire arrays by chemical etching and thermal oxidation, Nanotechnology 27 (2016) 165303.